Multiuser Decision-Feedback Equalization of Block-spread Multirate Transmissions for QoS Wireless Networking

Anastasios Stamoulis, Georgios B. Giannakis
Dept. of Electrical and Computer Engineering
University of Minnesota, Minneapolis, MN 55455
stamouli,georgios@ece.umn.edu

Abstract— **Multiuser Decision Feedback (DF) receivers can be employed to improve the bit error performance at the physical layer of wireless networks. Given a wireless network framework capable of utilizing "capacity" gains at the physical layer, DF receivers elevate the provisioned QoS guarantees. This paper develops closed-form FIR DF receivers suitable for multirate multipath transparent CDMA transmissions with block spreading codes. Capitalizing on the multiuser elimination capabilities of our CDMA framework, our DF receivers outperform both the linear and the successive interference canceller (SIC) receivers. Simulations illustrate the merits of our designs.**

I. Introduction

QoS Wireless Networking, similar to its wireline counterpart, aims to provide throughput, delay, and bit error rate (BER) guarantees. Unlike wireline networking, wireless networking has to cope with the wireless channel idiosyncrasy, which manifests itself as "variable capacity": time- and frequency-selective fading along with multiuser interference (MUI) lead to increased BER, which in turn necessitates packet retransmissions; hence, to decreased "goodput" and increased delay. To combat the intrinsic impairment of the wireless physical medium, one should exploit all available forms of diversity; on the other hand, provision of QoS guarantees in a wireless environment calls for the joint design of the network, link, and physical layers. As shown in [1], such a joint design leads to improved performance at both the network and the physical layers. Herein, we further improve the BER performance at the physical layer by developing block FIR multiuser decision feedback (DF) receivers as a replacement for the linear receivers of [1,2]. In this work, we focus on the merits of our designs at the physical layer. Our paper is organized as follows. In Section II we motivate the study of DF receivers by explaining the design philosophy of [1], which enables DF-induced performance improvements to be utilized for QoS provision. Then, in Section III we describe the physical layer of [1], and in Section IV we develop our multi-user DF receivers. In Section V we illustrate the BER improvements through simulations, and in Section VI we summarize and give pointers to future research.

Work in this paper was supported by the NSF Wireless Initiative grant no. 99-79443.

II. Provision of QoS in Wireless Networks

We look at a cellular environment where packets are transmitted between the mobile users and the basestation. The overall system performance, in terms of throughput, delay, and packet error probability, depends critically upon the performance at the network, data link, and physical layers. At the network layer, throughput and delay guarantees can be realized through a Generalized Processor Sharing scheduler [3]: every user m is associated with a service dependent weight ϕ_m; the amount of bandwidth BW_m allocated to user m is $\mathrm{BW}_m = \phi_m \mathrm{BW} / \sum_{\mu\in\mathcal{A}} \phi_\mu$, where BW is the overall bandwidth and $\mathcal{A}$ is the set of active users. At the data link layer, throughput and delay guarantees are ensured by a two-phase demand assignment medium access control (MAC) protocol. During the first phase, each user m notifies the base station about its intention to transmit and the requested ϕ_m; the base station notifies each user about the corresponding code assignment. During the second phase, users rely on these codes to transmit (at possibly different rates) multimedia information. At the physical layer, BER and throughput guarantees are provided by a multirate multipath transparent Generalized Multi-Carrier (GMC) CDMA framework. As proved in [1,2], the joint design of user codes and receivers guarantees deterministic multiuser elimination and deterministic symbol recovery regardless of the underlying FIR physical channel[1]. As we explain in the next section, the code assignment procedure ties the network, MAC, and physical layer together; as a result, BER improvement at the physical layer evinces itself as throughput increase at the network layer. This is exactly our motivation for the development of GMC-CDMA DF receivers.

III. Physical Layer

First we provide a high-level view of our system, and then we will proceed to a more detailed description.

[1]As discussed in Section III, as long as there is a bound on the order of the FIR channel, the physical layer guarantees symbol recovery (in the absence of noise); hence, the term "multipath transparent". Note also that an estimate of the order of the channel depends on the symbol rate, the carrier frequency and the environment type, e.g., urban, hilly, indoor, etc. (see, e.g., [4,5]).

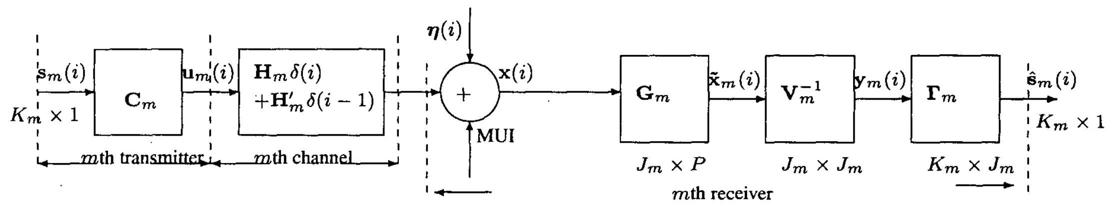

Fig. 1. Block model

High Level View Fig. 1 depicts the uplink channel of our GMC-CDMA system. The user m uses his assigned code matrix $\mathbf{C}_m$ to transmit blocks $\mathbf{s}_m(i)$ of size K_m. Through the code $\mathbf{C}_m$, the $K_m \times 1$ vector $\mathbf{s}_m(i)$ is mapped to a $P \times 1$ vector $\mathbf{u}_m(i) = \mathbf{C}_m\mathbf{s}_m(i)$ which is transmitted over the channel; we note that block-spreading enables multirate transmissions by altering K_m. The channel $\{h(n)\}_{n=0}^{L}$, which is assumed to be FIR of order L, is represented by the matrices $\mathbf{H}_m$ and $\mathbf{H}'_m$. The received block $\mathbf{x}(i)$ contains MUI and additive noise $\boldsymbol{\eta}(i)$:

$$\mathbf{x}(i) = \sum_{\mu=0}^{M-1} \left(\mathbf{H}_\mu \mathbf{C}_\mu \mathbf{s}_\mu(i) + \mathbf{H}'_\mu \mathbf{C}_\mu \mathbf{s}_\mu(i-1)\right) + \boldsymbol{\eta}(i)\,. \quad (1)$$

The receiver removes MUI using the filterbanks described by the matrices $\mathbf{G}_m$ and $\mathbf{V}_m^{-1}$. In [1, 2, 6], the transmitted data $\mathbf{s}_m(i)$ are recovered using the zero-forcing equalizer $\boldsymbol{\Gamma}_m$ (as we explain later on, the channel matrix is full column rank, which guarantees the existence of the pseudo-inverse $\boldsymbol{\Gamma}_m$). Herein, we develop DF receivers to improve the BER performance. We base our DF receivers on the results of [7], which derived closed-form block FIR DF receivers for the single user case. It turns out that these DF receivers can be used in our multiuser environment, because the joint design of the code $\mathbf{C}_m$ and the receiver $\mathbf{G}_m$ renders the multiuser environment to that of a single-user.

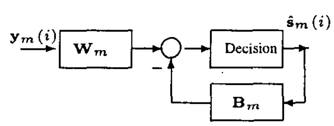

Fig. 2. GMC-CDMA DF receiver

Fig. 2 depicts the structure of the DF receiver, which consists of the feedforward filterbank represented by the $K_m \times J_m$ matrix $\mathbf{W}_m$, the decision making device, and the feedback filterbank represented by the $K_m \times K_m$ matrix $\mathbf{B}_m$. The feedforward filter is responsible for eliminating ISI from "future" symbols within the current block, whereas the feedback filter is responsible for eliminating ISI from "past" symbols.

Detailed View Signals, codes, and channels of the uplink CDMA channel are represented by samples of their complex envelopes taken at the chip rate. The data symbol sequence of the m-th user is denoted by $s_m(k)$ and through serial-to-parallel converters is grouped into blocks of K_m symbols $\mathbf{s}_m(i){:=}[s_m(iK_m)\ldots s_m(iK_m + K_m - 1)]^T$. Using the order $P-1$ FIR precoding filterbank $\{c_{m,k}(n)\}_{k=0}^{K_m-1}$, the block $\mathbf{s}_m(i)$ is mapped to a block $\mathbf{u}_m(i)$ of $P > K_m$ chips: $\mathbf{u}_m(i) = \mathbf{C}_m\mathbf{s}_m(i)$, where the (n,k)th entry of the $P \times K_m$ matrix $\mathbf{C}_m$ is $c_{m,k}(n)$.

The coded[2] chip sequence $u_m(n)$ passes through the discrete-time equivalent baseband channel $h_m(n)$, which is assumed to be of order $\leq L$ (a common assumption in quasi-synchronous CDMA systems [6]). The impulse response $h_m(n)$ models multipath, transmit-receive filters, and the mth user's asynchronism in the form of delay factors [6]. The chip-sampled sequence is: $x(n) = \sum_{m=0}^{M-1} x_m(n) + \eta(n)$, where: $x_m(n){:=}\sum_{j=0}^{L} h_m(j)u_m(n-j)$, and $\eta(n)$ is the additive noise. Similar to OFDM, the first L symbols of the received block are discarded at the receiver to eliminate IBI. The received $P\times 1$ vector $\mathbf{x}(i){:=}[x(iP)\ldots x(iP{+}P{-}1)]^T$ in AGN $\boldsymbol{\eta}(i){:=}[\eta(iP)\ldots\eta(iP+P-1)]^T$ is given by (1). The $P \times P$ Toeplitz (convolution) matrix $\mathbf{H}_m$ has first row $(\ h(0)\ \ldots\ 0\ )$, first column $(\ h(0)\ \ldots\ h(L)\ 0\ \ldots\ 0\ )^T$ and models the intersymbol interference (ISI) within the symbols of a block. The $P \times P$ Toeplitz matrix $\mathbf{H}'_m$ has first row $(0\ldots 0\,h(L)\ldots h(1))$ and first column $\mathbf{0}_{P\times 1}$, and is responsible for the interblock interference (IBI).

At the receiver end, recovery of the transmitted block $\mathbf{s}_m(i)$ entails two actions: i)elimination of MUI, and ii)elimination of multipath induced ISI (within a block). These actions are implemented by filterbanks or DSP processors performing block processing that amounts to multiplying the received blocks by the matrices $\mathbf{G}_m$, $\mathbf{V}_m^{-1}$, $\mathbf{W}_m$, and $\mathbf{B}_m$. The first stage of the receiver for user m consists of J_m parallel filters $\{g_{m,j}(p)\}_{j=0}^{J_m-1}$, each of length P. The taps of the filters are given by the entries of the $J_m \times P$ matrix $\mathbf{G}_m$ with (j,p) entry $[\mathbf{G}_m]_{j,p} = g_{m,j}(p)$. The matrix $\mathbf{G}_m$ maps the block $\mathbf{x}(i)$ to an MUI-free block $\mathbf{y}_m(i)$:

$$\mathbf{y}_m(i) \quad = \quad \mathbf{G}_m\mathbf{H}_m\mathbf{C}_m\mathbf{s}_m(i) + \mathbf{G}_m\boldsymbol{\eta}(i)$$

[2] We note that error-control codes are not precluded from our GMC-CDMA system. A possible channel encoder should precede the block-spreading operation that $\mathbf{C}_m$ implements, and either operate before the S/P converter (e.g., as in the case of a convolutional code) or after the S/P converter (e.g., as in the case of a Reed-Solomon code).

$$+ \underbrace{\sum_{\mu=0,\mu\neq m}^{M-1} \mathbf{G}_m \mathbf{H}_\mu \mathbf{C}_\mu \mathbf{s}_\mu(i)}_{\text{MUI}} . \quad (2)$$

One of the fundamental characteristics of our physical layer framework is that code orthogonality is guaranteed irrespective of the FIR multipath environment. In other words, $\mathbf{C}_m$, $\mathbf{G}_m$ are selected such that MUI is eliminated in (2) and the matrix $\mathbf{G}_m\mathbf{H}_m\mathbf{C}_m$ is full rank irrespective of the channel $\mathbf{H}_m$. The aforementioned requirements are satisfied by the following procedure [1,6]: each user m is assigned J_m complex numbers $\rho_{m,j}$ $(0 \leq j \leq J_m - 1)$, which are termed user m's "signature points". The number of signature points is selected such that:

$$P = \sum_{m=0}^{M-1} J_m + L \, , \; K_m = J_m - L, \; 0 \leq m \leq M-1 \, . \quad (3)$$

The signature points are used to construct the code matrix $\mathbf{C}_m$ with (p, k)th entry $(0 \leq p \leq P-1, 0 \leq k \leq K_m - 1)$:

$$c_{m,k}(p) = \mathcal{A}_m \sum_{j=0}^{J_m-1} \rho_{m,j}^{-P+1+p-k} \, , \quad (4)$$

where $\mathcal{A}_m$ is a constant controlling transmitted power. The receiver matrix $\mathbf{G}_m$ is built out of the coefficients of the following Lagrange polynomials $(0 \leq j \leq J_m - 1)$ [6]:

$$\sum_{n=0}^{P-L-1} [\mathbf{G}_m]_{j,(P-1-n)} z^{-n} := \prod_{\substack{\mu=0,\lambda=0 \\ (\mu,\lambda)\neq(m,j)}}^{M-1,J_m-1} \frac{1-\rho_{\mu,\lambda} z^{-1}}{1-\rho_{\mu,\lambda}\rho_{m,j}^{-1}}$$
$$[\mathbf{G}_m]_{j,p} := 0 \, , \; 0 \leq p \leq (L-1) \quad (5)$$

Then, it is proved in [1,6] that the MUI/IBI free data for user m are contained in:

$$\tilde{\mathbf{x}}_m(i) := \mathcal{A}_m \begin{pmatrix} H_m(\rho_{m,0}) S_m(i;\rho_{m,0}) \\ \vdots \\ H_m(\rho_{m,J_m-1}) S_m(i;\rho_{m,J_m-1}) \end{pmatrix} + \mathbf{G}_m \boldsymbol{\eta}(i) \, , \quad (6)$$

where: $H_m(z) := \sum_{l=0}^{L} h_m(l) z^{-l}$, and
$S_m(i;z) := \sum_{k=0}^{K_m-1} s_m(iK_m + k) z^{-k}$. □

To recover the transmitted symbols, let $\mathbf{V}_m$ be a $J_m \times J_m$ matrix with its (i,j)-th entry given by $\mathcal{A}_m \rho_{m,i}^{-j}$. Because MUI has been eliminated from (6), $\mathbf{V}_m^{-1}$ can be applied[3] to $\tilde{\mathbf{x}}_m(i)$ to obtain the single input single output (SISO) vector model:

$$\mathbf{y}_m(i) = \tilde{\mathbf{H}}_m \boldsymbol{\Theta}_m \mathbf{s}_m(i) + \boldsymbol{\eta}_m(i) \, , \quad (7)$$

where: $\tilde{\mathbf{H}}_m$ is a $J_m \times J_m$ Toeplitz matrix (defined in the same way as $\mathbf{H}_m$), $\boldsymbol{\Theta}_m := [\mathbf{I}_{K_m \times K_m} \; \mathbf{0}_{K_m \times L}]^T$, and $\boldsymbol{\eta}_m(i) := \mathbf{V}_m^{-1} \mathbf{G}_m \boldsymbol{\eta}(i)$.

[3] Distinct signature points $\rho_{m,j}$ guarantee invertibility of the Vandermond matrix $\mathbf{V}_m$.

It follows from (7) that our GMC-CDMA system is converted to M parallel single-user systems. Any single user equalizer $\boldsymbol{\Gamma}_m$ can then be applied to $\mathbf{y}_m(i)$ in order to recover the symbols $\mathbf{s}_m(i)$; e.g., $\boldsymbol{\Gamma}_m = \tilde{\mathbf{H}}_m^\dagger$ corresponds to a zero-forcing equalizer. Note that $\tilde{\mathbf{H}}_m$ is full-column rank, which guarantees the existence of the pseudo-inverse $\tilde{\mathbf{H}}_m^\dagger$. We underline that the ability to equalize the frequency-selective channel is exactly what renders our GMC-CDMA framework multipath-transparent. Furthermore, the ability to assign a different number of signature points per user enables our GMC-CDMA framework to support multi-rate/packet-level services by selecting P sufficiently large.

Making the transmission/reception scheme multipath transparent comes with a price to be paid. From (3), it follows that while user m is assigned $J_m = K_m + L$ signature points, the L signature points are used to annihilate the L possible nulls of the physical channel, but only K_m are used for transmission of information symbols. However, if the channel for every user is known, then the signature points $\rho_{m,j}$ $(0 \leq j \leq J_m - 1)$ can be selected such that $H_m(\rho_{m,j}) \neq 0$. In this case, K_m can be set equal to J_m, which minimizes the redundancy at the physical layer, and guarantees recovery of the transmitted data without the inversion of the channel matrix [6].

IV. DF RECEIVER

As we saw in Section III, our MUI eliminating codes render the multi-user channel equivalent to M independent single-user channels. As (7) suggests, the recovery of the users' transmitted symbols amounts to inverting the channel matrix $\mathbf{H}_m$ using a zero-forcing matrix inverse or an MMSE-receiver matrix ("Wiener inverse"). Indeed, at high signal-to-noise ratios (SNR), a linear ZF equalizer structure is expected to equalize the channel perfectly. However, BER performance can be improved (especially at low SNR) in two ways. First, by exploiting the finite alphabet of the input and taking into account decisions about the symbols in the same block. Second, by whitening the noise at the input of the decision device. Noise whitening makes symbol-by-symbol detection optimal; thus, symbol-by-symbol detection is desirable from a practical point of view. Therefore, the question which naturally arises is whether there exists a linear receiver capable of making the noise samples independent at the input of the decision device. In single-user block transmission systems, if CSI is available at the transmitter, then joint design of the linear transmit/receive filterbanks (as a function of the channel and the noise autocorrelation) assures symbol recovery with white noise at the input of the decision device [8]. These results could be readily applied to our multiuser framework because the outer code transforms the multiuser channel to a single-user channel. Unfortunately, CSI is required at the transmitter. Fortunately, with a DF receiver, CSI is not required at the transmitter. Hence, both noise whitening and exploitation of finite alphabet/past decisions can be realized through our block zero-forcing (ZF) DF that we develop next.

The decision feedback equalizer (see Fig. 2) consists of the feedforward filterbank represented by the $K_m \times J_m$ matrix $\mathbf{W}_m$, the decision device and the feedback filterbank represented by the $K_m \times K_m$ matrix $\mathbf{B}_m$. The feedforward filter is responsible for eliminating ISI from "future" symbols within the current block, whereas the feedback filter is responsible for eliminating ISI from "past" symbols. To derive the settings of the DF receiver, let us define the $K_m \times 1$ vectors: $\mathbf{z}_m(i):=[\, z_m(iK_m)\; z_m(iK_m+1) \ldots z_m(iK_m+K_m-1)\,]^T$, and $\tilde{\mathbf{s}}_m(i):=[\, \tilde{s}_m(iK_m)\; \tilde{s}_m(iK_m+1) \ldots \tilde{s}_m(iK_m+K_m-1)\,]^T$. Based on (7), and Fig. 2 we obtain:

$$\begin{aligned} \mathbf{z}_m(i) &= \mathbf{W}_m\tilde{\mathbf{H}}_m\mathbf{\Theta}_m\mathbf{s}_m(i) + \mathbf{W}_m\boldsymbol{\eta}_m(i) && \text{(8a)} \\ \tilde{\mathbf{s}}_m(i) &= \mathbf{z}_m(i) - \mathbf{B}_m\hat{\mathbf{s}}_m(i) && \text{(8b)} \\ \hat{\mathbf{s}}_m(i) &= Q(\tilde{\mathbf{s}}_m(i)) && \text{(8c)} \end{aligned}$$

where $Q(\cdot)$ is the quantizer used by the decision device.

Symbol-by-symbol detection is rendered optimal by allowance for "successive cancellation", and whitening of the noise at the input of the decision device. Additionally, the ZF-DFE receiver should guarantee zero-forcing: in the absence of noise and under the assumption of correct past decisions, the decision statistic should be equal to the transmitted data: $\tilde{\mathbf{s}}_m(i) = \mathbf{s}_m(i) = \hat{\mathbf{s}}_m(i)$. In view of (8), the latter translates the ZF requirement to:

$$\mathbf{W}_m\tilde{\mathbf{H}}_m\mathbf{\Theta}_m = \mathbf{B}_m + \mathbf{I}_{K_m}.$$

Because past decisions are assumed correct, the noise at the input of the decision device is $\mathbf{W}_m\boldsymbol{\eta}_m(i)$, and in order to whiten it we select $\mathbf{W}_m$ such that:

$$\mathbf{W}_m\mathbf{R}_{\eta_m\eta_m}\mathbf{W}_m^{\mathcal{H}} = \text{a diagonal matrix},$$

where $\mathbf{R}_{\eta_m\eta_m}:=E\{\boldsymbol{\eta}_m(i)\boldsymbol{\eta}_m^{\mathcal{H}}(i)\}$ is the autocorrelation of the noise. Finally, "successive cancellation" is made possible by selecting the feedback matrix $\mathbf{B}_m$ strictly upper triangular. By successive cancellation we mean that for every block indexed by i, the (K_m-1)st symbol is recovered first; then the estimate $\hat{s}_m(iK_m+K_m-1)$ is weighted by the last column of $\mathbf{B}_m$ and is removed from $\mathbf{z}_m(i)$ so that the remaining symbols can be recovered. The (K_m-2)nd symbol is recovered next, and the estimate $\hat{s}_m(iK_m+K_m-2)$ is removed from $\mathbf{z}_m(i)$. This procedure is carried out until all the symbols of the current block i have been estimated.

It can be verified by direct substitution that the following assignment of $(\mathbf{W}_m, \mathbf{B}_m)$ satisfies the requirements for the ZF-DFE receiver:

$$\begin{aligned} \mathbf{W}_m &= \mathbf{D}_m^{-1}\mathbf{U}_m^{-\mathcal{H}}(\tilde{\mathbf{H}}_m\mathbf{\Theta}_m)^{\mathcal{H}}\mathbf{R}_{\eta_m\eta_m}^{-1} && \text{(9a)} \\ \mathbf{B}_m &= \mathbf{U}_m - \mathbf{I}_{K_m}, && \text{(9b)} \end{aligned}$$

where $\mathbf{U}_m$ is an upper triangular matrix with unit diagonal given by the Cholesky factorization of the matrix

$$(\tilde{\mathbf{H}}_m\mathbf{\Theta}_m)^{\mathcal{H}}\mathbf{R}_{\eta_m\eta_m}^{-1}(\tilde{\mathbf{H}}_m\mathbf{\Theta}_m) = \mathbf{U}_m^{\mathcal{H}}\mathbf{D}_m\mathbf{U}_m,$$

with $\mathbf{D}_m$ a diagonal matrix.

One could also trade-off ISI elimination for noise suppression using a DF receiver which minimizes the minimum mean square error (MMSE) at the input of the decision device. The MMSE-DF receiver takes into account the autocorrelation of the input symbols $\mathbf{R}_{s_ms_m}:=E\{\mathbf{s}_m(i)\mathbf{s}_m^{\mathcal{H}}(i)\}$, and the autocorrelation of the MUI/IBI free data $\mathbf{R}_{y_my_m}:=E\{\mathbf{y}_m(i)\mathbf{y}_m^{\mathcal{H}}(i)\} = (\tilde{\mathbf{H}}_m\mathbf{\Theta}_m)\mathbf{R}_{s_ms_m}(\tilde{\mathbf{H}}_m\mathbf{\Theta}_m)^{\mathcal{H}} + (\mathbf{V}_m^{-1}\mathbf{G}_m)\mathbf{R}_{\eta\eta}(\mathbf{V}_m^{-1}\mathbf{G}_m)^{\mathcal{H}}$. The settings of the MMSE-DF receiver, whose derivation we omit due to lack of space, are given by:

$$\begin{aligned} \mathbf{B}_m &= \mathbf{U}_m - \mathbf{I}_m && \text{(10a)} \\ \mathbf{W}_m &= \mathbf{U}_m\mathbf{R}_{s_my_m}\mathbf{R}_{y_my_m}^{-1}, && \text{(10b)} \end{aligned}$$

where $\mathbf{U}_m$ is an upper triangular matrix with unit diagonal given by the Cholesky factorization of

$$\mathbf{R}_{s_ms_m}^{-1} + (\tilde{\mathbf{H}}_m\mathbf{\Theta}_m)^{\mathcal{H}}\mathbf{R}_{\eta_m\eta_m}^{-1}(\tilde{\mathbf{H}}_m\mathbf{\Theta}_m) = \mathbf{U}_m^{\mathcal{H}}\mathbf{D}_m\mathbf{U}_m,$$

with $\mathbf{D}_m$ a diagonal matrix.

We also study the "successive decorrelator[4]" of [9, pp. 370–382] (which corresponds to $K_m = 1$), and we extend it to our multiple rate framework ($K_m \geq 1$). The successive decorrelator performs symbol recovery and MUI elimination simultaneously[5]; it is built as a function of the channel and the code matrices as follows. As we have seen, discarding the first L symbols of the received block $\mathbf{x}(i)$ produces the IBI-free block $\mathbf{y}(i):=\mathbf{R}_{cp}\mathbf{x}(i) + \mathbf{R}_{cp}\boldsymbol{\eta}(i)$, with $\mathbf{R}_{cp}:=[\mathbf{0}_{(P-L)\times L}\; \mathbf{I}_{(P-L)\times(P-L)}]$. Hence, we can write:

$$\begin{aligned} \mathbf{y}(i) &= [\mathbf{R}_{cp}\mathbf{H}_0\mathbf{C}_0 \ldots \mathbf{R}_{cp}\mathbf{H}_{M-1}\mathbf{C}_{M-1}]\begin{bmatrix} \mathbf{s}_0(i) \\ \vdots \\ \mathbf{s}_{M-1}(i) \end{bmatrix} \\ &\quad + \mathbf{R}_{cp}\boldsymbol{\eta}(i) \\ &:= \mathbb{H}\tilde{\mathbf{s}}(i) + \mathbf{R}_{cp}\boldsymbol{\eta}(i), && \text{(11)} \end{aligned}$$

where the $(P-L) \times 1$ vector $\tilde{\mathbf{s}}(i)$ contains the transmitted symbols of all the users, and the $(P-L) \times (P-L)$ matrix

$$\mathbb{H}:=[\mathbf{R}_{cp}\mathbf{H}\mathbf{C} \ldots \mathbf{R}_{cp}\mathbf{H}_{M-1}\mathbf{C}_{M-1}]$$

contains the channels-codes corresponding to each user.

Given the similarity between (7) and (11), we can proceed as before and design a ZF-DF receiver (SIC) which recovers all the transmitted symbols. The feed-forward and feedback filters $\mathbf{W}, \mathbf{B}$ are given by:

$$\mathbf{B} = \mathbf{U} - \mathbf{I}_{P-L},\; \mathbf{W} = \mathbf{D}^{-1}\mathbf{U}^{-1}(\mathbb{H})^{\mathcal{H}},$$

where $\mathbf{U}$ is upper triangular with unit diagonal given by the Cholesky factorization $\mathbb{H}^{\mathcal{H}}\mathbb{H} = \mathbf{U}^{\mathcal{H}}\mathbf{D}\mathbf{U}$, with $\mathbf{D}$ a diagonal matrix.

The basic difference between the SIC and our multiuser DF receivers is that our multiuser DF receivers exploit the mutual orthogonality of the user-codes and, as a result, need to cope with only the inversion of the channel and the suppression of the noise. On the other hand, the SIC attempts to combat MUI and ISI simultaneously. As indicated in the Simulations section, the latter does not appear to be the best strategy for our

[4] Often referred to as Successive Interference Canceler (SIC).

[5] Hence, it does not use the matrices $\mathbf{G}_m, \mathbf{V}_m^{-1}$.

system. Before we present our Simulations results, we comment on how possible BER improvements at the physical layer can be made visible to the network layer.

Code Assignment The m-th user's effective transmission rate is determined by the number K_m of symbols which are spread by the code $\mathbf{C}_m$ during the transmission phase. For a fixed upper bound L on the maximum channel order, the number $K_m = J_m - L$ is in turn determined by the number of signature points J_m that are allocated to user m. Supposing a constant transmission phase, the block size P is fixed, and the numbers J_m $(0 \leq m \leq M-1)$ should be selected such that fair bandwidth allocation is achieved. This is accomplished by using:

$$J_m = \lfloor \tfrac{\mathrm{BW}_m}{\mathrm{BW}}(P-L) \rfloor ,$$

which guarantees that during the transmission phase, user m will be allocated his/her fair share of the bandwidth. Note at this point that the truncation error is insignificant, because P is in the order of multiple packet lengths: for wireless ATM, the cell is 424 bits, which implies that indeed transmission rates of arbitrarily fine resolution are achieved.

V. SIMULATIONS

Our simulations focus on the physical layer performance of our DF receivers. We refer the reader to [10] for a study which shows that indeed improved BER performance at the physical layer is reflected as throughput increase at the network layer. Fig. 3 shows the BER performance for a system with $M = 3$ users, $P = 46$, $L = 4$. Each user has $\phi = 1$ (equal rate case) which yields $K_m = 10$. The BER curves depict the average of 50 channels with random Gaussian coefficients. We study the performance of 4 types of receivers: the linear receiver of [1,2], the ZF-DF and MMSE-DF receiver, and the successive decorrelator. From Fig. 3 we can deduce the superiority of our DF receivers. Moreover, we see the suboptimality of the SIC, which does not manage to separate the users completely and as a result it yields higher BER than our DF receivers. The same applies in the following two test cases. Fig. 4 depicts the performance of the aforementioned receivers when $L = 11$, $M = 3$, and $P = 104$. The random channels are modeled after the first 12 taps of "Channel A" of [11], which corresponds to a typical office environment[6]. Finally, Fig. 5 depicts the performance in the case of $L = 2$, $P = 74$, $M = 4$; 2 high-rate users have $\phi_{hr} = 2$, and 2 low-rate users have $\phi_{lr} = 1$. As in the previous cases, our multiuser DF receivers exhibit improved BER performance.

[6]According to [11], the Taps delays are `Delays=[0 10 20 30 40 50 60 70 80 90 110 140 170 200 240 290 340 390]` (in ns), and the corresponding average relative powers are `AvgRelativePower=[0 -0.9 -1.7 -2.6 -3.5 -4.3 -5.2 -6.1 -6.9 -7.8 -4.7 -7.3 -9.9 -12.5 -13.7 -18.0 -22.4 -26.7]` (in dB) – the first 12 taps capture the 90% of the energy.

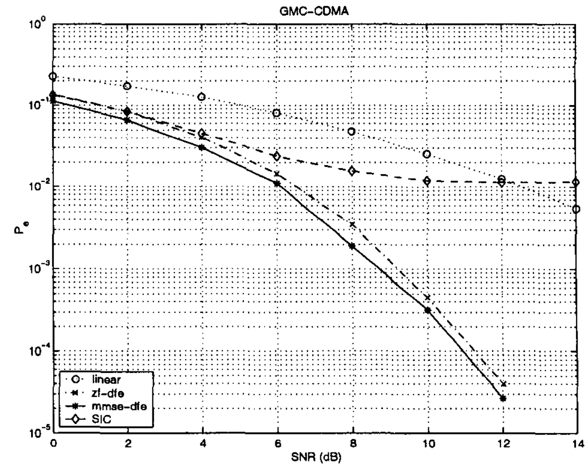

Fig. 3. Receiver Performance, $L = 4$

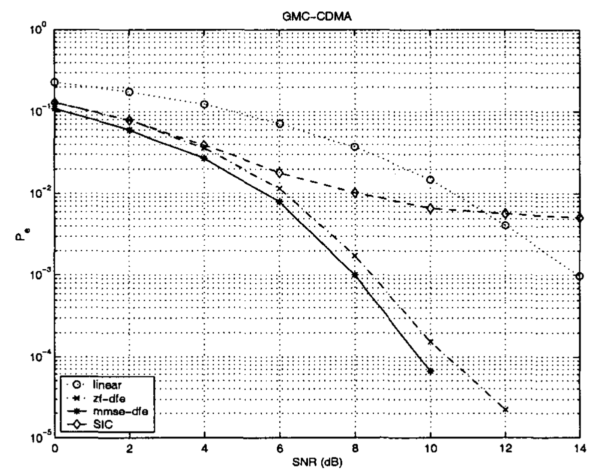

Fig. 4. Receiver Performance, $L = 11$

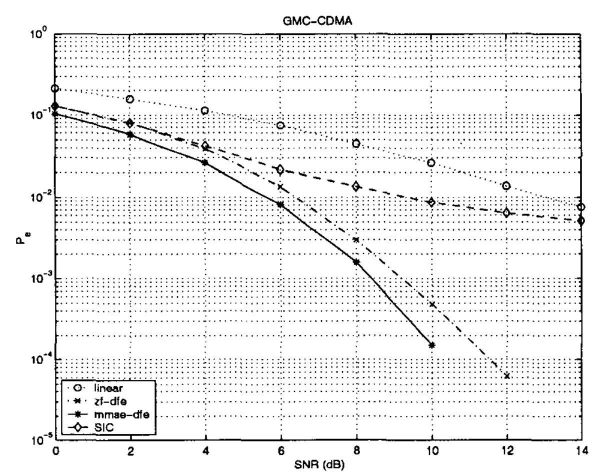

Fig. 5. Receiver Performance, $L = 2$, High/Low-Rate Case

VI. CONCLUSIONS

In this paper we have presented multi-user DF receivers for a block-spread multirate CDMA system. Capitalizing on the mutual code orthogonality of the underlying system, our DF receivers, in order to recover the transmitted symbols, need to cope only with ISI elimination and noise suppression. Furthermore, our DF receivers exploit the block nature of wireless transmissions and employ FIR structures which implement exactly closed-form solutions for ZF and MMSE equalization. As a result, our designs exhibit improved BER compared to that of the linear and the SIC equalizer. Future work includes the design of multi-element DF receivers which utilize multiple receive antennas at the basestation (see, e.g., [12] and references therein).

REFERENCES

[1] A. Stamoulis and G. B. Giannakis, "Packet Fair Queueing Scheduling Based on Multirate Multipath-Transparent CDMA for Wireless Networks," in *Proc. of INFOCOM2000*, Tel Aviv, Israel, March 2000, pp. 1067–1076.

[2] Z. Wang and G.B. Giannakis, "Block Precoding for MUI/ISI-Resilient Generalized Multi-carrier CDMA with Multirate Capabilities," in *ICC'2000*, 2000.

[3] A. K. Parekh and R. G. Gallager, "A Generalized Processor Sharing Approach to Flow Control in Integrated Services Networks: The Single-Node Case," *IEEE/ACM Transactions on Networking*, vol. 1, no. 3, pp. 344–357, June 1993.

[4] A.J. Van Der Veen, "Algebraic methods for deterministic blind beamforming," *Proceedings of the IEEE*, vol. 86, no. 10, pp. 1987–2008, October 1998.

[5] T.S. Rappaport, *Wireless communications : principles and practice*, Prentice Hall, 1996.

[6] G. B. Giannakis, Z. Wang, A. Scaglione, and S. Barbarossa, "AMOUR — Generalized Multicarrier Transceivers for Blind CDMA regardless of Multipath," *IEEE Trans. on Communications*, 2000 (to appear).

[7] A. Stamoulis, G.B. Giannakis, and A. Scaglione, "Block FIR Decision-Feedback Equalizers for Filterbank Precoded Transmissions with Blind Channel Estimation Capabilities," *IEEE Trans. on Communications*, 2000 (to appear).

[8] A. Scaglione, G. B. Giannakis, and S. Barbarossa, "Redundant filterbank precoders and equalizers, Part I: Unification and optimal designs," *IEEE Trans. on Signal Processing*, vol. 47, no. 7, pp. 1988–2006, July 1999.

[9] S. Verdú, *Multiuser Detection*, Cambridge University Press, 1998.

[10] A. Stamoulis, Z. Liu, and G.B. Giannakis, "Deterministic QoS Wireless Networking based on Multirate Space-Time CDMA," in *Proc. of INFOCOM2001*, (submitted).

[11] ETSI Normalization Commitee, "Channel Models for HIPERLAN/2 in different indoor scenarios," Norme ETSI, document 3ERI085B, European Telecommunications Standards Institute, Sophia-Antipolis, Valbonne, France, 1998.

[12] T. Fulghum and A. Duel-Hallen, "Adaptive multielement DFE receivers for narrowband multiuser detection," in *VTC '98. 48th IEEE Vehicular Technology Conference*, Ottawa, Ont., Canada, May 1998, vol. 1, pp. 41–45.